Whitmarsh, R.B., Sawyer, D.S., Klaus, A., and Masson, D.G. (Eds.), 1996
Proceedings of the Ocean Drilling Program, Scientific Results, Vol. 149

36. SERPENTINIZED PERIDOTITE BRECCIA AND OLISTOSTROME ON BASEMENT HIGHS OF THE IBERIA ABYSSAL PLAIN: IMPLICATIONS FOR TECTONIC MARGIN EVOLUTION[1]

M.C. Comas,[2] M. Sánchez-Gómez,[2] G. Cornen,[3] and E. de Kaenel[4]

ABSTRACT

Rock samples from Sites 897 and 899 were examined to determine the origin of the early Cretaceous lithologic complex recovered on the top of basement highs in the Iberia Abyssal Plain. Samples studied belong to sedimentary rocks, serpentinized peridotite breccias, metabasites, and mafic rocks. The sedimentary rocks correspond to reworked elements of previously consolidated pelagic and turbidite facies and to unconsolidated pelagic marly sediments. Nannofossil assemblages from the sedimentary rocks indicate a similar early Aptian age for this lithologic complex at the two sites. Ultramafic rocks present in breccias (boulders, clasts, and fragments) vary in composition, and range from peridotite and serpentinized peridotite to altered serpentinite. Chlorite-rich metabasites are minor components in the breccia. Mafic rocks are mainly associated with sediments and occur at both sites. They comprise basaltic lava, undeformed microgabbros, and sheared amphibolite. A polyphase deformation that resulted in cataclastic fabrics affected the serpentinized peridotite breccias. Cataclastic lineation, flow, and foliation structures are present in the breccia fabrics and, consequently, the serpentinized peridotite breccia is considered a tectonic cataclasite. The igneous-sedimentary complex is interpreted as olistostrome(s) that accumulated in a basin-plain setting. Breccia intervals are interpreted as olistoliths or blocks from former cataclastic breccias. The olistostrome, involving sedimentary, ultramafic, and mafic rocks, is thought to be derived from a lower Aptian marginal ridge related to a probable transform fault boundary (the Figueiro Transform Fault), between the Galicia Margin and the Iberia Abyssal Plain at that time. The marginal ridge could have exposed serpentinized peridotites, serpentinized peridotite cataclastic breccias, mafic rocks, and older sediments to the seafloor. Cataclastic breccias and other fault rocks included in the olistostrome are interpreted as mainly originating from wrench tectonics in the transform fault zone, which probably also involved hydrothermal activity and seismicity. The activity of the Figueiro Transform Fault at the Iberia Abyssal Plain/Galicia Margin boundary can be restricted to the time between the development of the transitional crust (about 130 km wide) and early stages of seafloor spreading in the Iberia Abyssal Plain, and the breakup of the Galicia Margin; that is, from about late Hauterivian (129 Ma) to latest Aptian-early Albian (about 110 Ma). Post-rift normal faulting, which probably occurred at any time after the Late Aptian and before the latest Cretaceous or Paleogene, affected the crust at the ocean/continent transition of the Iberia Abyssal Plain and led to fault-bounded basement highs, on top of which the Aptian olistostromes were encountered.

INTRODUCTION

The western continental margin of the Iberian peninsula (Fig. 1) has the attributes of a sediment-starved, non-volcanic rifted margin. It is traditionally divided from north to south into three distinct segments in which rifting and drifting stages occurred at different times. The onset of the breakup or seafloor spreading within the three segments becomes younger from south to north. In the Galicia Margin the breakup is considered to be post-M0 (about 110 Ma, latest Aptian-early Albian; Boillot, Winterer, Meyer, et al., 1987). In the Iberia Abyssal Plain (39°30'-41°N) the breakup is likely to have started before M3 (about 129 Ma, late Hauterivian) (Kent and Gradstein, 1986; Whitmarsh et al., 1990; Whitmarsh et al., 1993). Finally, in the Tagus Abyssal Plain the breakup is considered to have occurred between 134 Ma (Tithonian-Berriasian; Mauffret et al., 1989) and anomaly Mil, 136 Ma (Valanginian; Pinheiro et al., 1992).

Ocean Drilling Program Leg 149 was devoted to the investigation of the ocean/continent transition (OCT) in the Iberia Abyssal Plain (IAP) off Portugal, as this zone was believed to contain evidence that would enable us to construct satisfactory rifting models. The prime objective of Leg 149 was to drill and sample basement rocks along an east-west transect of sites across a transitional crust to the east of the ocean/continent boundary (Fig. 1; Sawyer, Whitmarsh, Klaus, et al., 1994). To allow substantial penetration of the acoustic basement, the sites were located over the crest of fault-bounded basement highs, which stretch out roughly parallel to the ocean/continent boundary. During Leg 149, the *JOIDES Resolution* drilled into the acoustic basement at Sites 897, 899, and 900.

At Site 897 we succeeded in penetrating and sampling up to 143 m of basement rocks composed of serpentinized, relatively undepleted peridotites from Hole 897C (5315.2 m water depth) and Hole 897D (5315.8 m water depth). Hole 897C was drilled to a depth of 744.9 mbsf, and Hole 897D to a depth of 837.2 mbsf. Friable serpentine breccia was found at the top of the peridotite basement in Hole 897C, and brecciated peridotites were encountered deeper in the peridotite basement in Hole 897D. Lower Aptian heterogeneous deposits, including clasts and boulders of serpentinized peridotite and serpentinite breccia, overlie the basement in both holes. The Shipboard Scientific Party (1994a) identified these heterogeneous deposits as Unit IV. Above the Lower Cretaceous deposits, a 650-m-thick Eocene to Pleistocene sedimentary sequence was cored and sampled.

At Site 899, Hole 899B (water depth of 5291 m) was drilled into the acoustic basement to a depth of 549.7 mbsf. However, in situ basement rocks were not encountered, and this hole yielded sedimentary samples over its total depth range. The 188 m of acoustic basement that was drilled in Hole 899B showed a heterogeneous lithological association including disrupted lower Aptian sediments associated with serpentinite breccias, boulders, and gouges, and fragments of basalts, microgabbros and sheared amphibolites. The Shipboard Sci-

[1]Whitmarsh, R.B., Sawyer, D.S., Klaus, A., and Masson, D.G. (Eds.), 1996. *Proc. ODP, Sci. Results,* 149: College Station, TX (Ocean Drilling Program).
[2]Instituto Andaluz de Ciencias de la Tierra, CSIC, and University of Granada, 18002 Granada, Spain. mcomas@goliat.ugr.es
[3]Laboratory of Petrology, University of Nantes, 2 rue de la Houssiniere, 44072 Nantes, cedex 03, France.
[4]Department of Geology, Florida State University, Tallahassee, FL 32306-3026, U.S.A.

entific Party (1994b) also identified this peculiar association as belonging to Unit IV. Overlying Unit IV, cores at Site 899 yielded a 370-m-thick sedimentary sequence that was Late Cretaceous to Late Pliocene in age (Sawyer, Whitmarsh, Klaus, et al., 1994).

The purpose of this study is to characterize Lower Cretaceous materials sampled at Sites 897 and 899 as products of synsedimentary tectonics and to determine the fabric and origin of the serpentinized peridotite breccia. Our analysis of the breccias focuses mainly on those recovered at Site 899.

Our results indicate that the fabric of these breccias originated from cataclastic processes related to the brittle fracturing of former serpentinized peridotite rocks. We interpret the whole lithologic complex as having accumulated from a contemporaneously active, major fault escarpment to the north of the Iberia Abyssal Plain.

SUMMARY OF EARLY CRETACEOUS SEDIMENTS AND AGES

Sediments and Sedimentary Environment

At Site 897 Early Cretaceous sediments (Fig. 2) were first sampled at the base of the designated Subunit IIIB (Shipboard Scientific Party, 1994a). In both Holes 897C and 897D, Subunit IIIB consists of gravity-flow deposits of poorly sorted, poorly cemented granule-to-pebble clayey conglomerate that grades upsection to granule conglomerate and very coarse-grained, lithic, ferruginous clayey sandstone, to sandy claystone. This fining-upward sequence occurred over an interval of about 20 m in Hole 897C and over 10 m in Hole 897D, and in both holes the sequence was dark reddish and variegated. Resedimented clasts included in the conglomerate have diverse lithology and facies: white limestone, micritic limestone, marlstones, dolomite, and varied turbiditic arkosic-to-lithic sandstones. Minor clasts of shallow carbonates included in conglomerates of Subunit IIIB are interpreted as reworked from a previous debris-flow deposit at the source area. Clasts and granules of basalt and serpentinized peridotites are present as minor components in the conglomerate and coarse sandstone. Because samples at the base of this conglomerate yield an early late Aptian age (see nannofossil assemblages below), and gravity flows accumulate over a very short time span, we consider the entire Subunit IIIB to be of early late Aptian age.

At Site 899, analogous reddish-variegated ferruginous conglomerate and coarse sandstone, including basalt pebbles, were sampled in one interval of about 1 m (Shipboard Scientific Party, 1994b). Although at Site 899 these lithologies are barren of nannofossils, the close correspondence between these facies and their counterpart sampled at Site 897, together with their similar position within the drilled sedimentary sequence, strongly suggests that they pertain to the same early late Aptian debris-flow event (Fig. 2).

Older Cretaceous sediments (Unit IV, Fig. 2), sampled down-section at Sites 897 and 899, consist of heterogeneous discrete sediment bodies mixed or intercalated with mafic and ultramafic rocks. Sediments in Unit IV yield an early Aptian age (see below). Unit IV was recovered in an interval of 28.6 m in Hole 897C, 38.6 m in Hole 897D and 188 m in Hole 899B (Sawyer, Whitmarsh, Klaus, et al., 1994). Our post-cruise biostratigraphy indicates the same age—early Aptian—for the complete sequence at both sites, which differs from those considered by the Shipboard Scientific Party (1994a, 1994b).

Major lithofacies present at both sites correspond to pelagic/hemipelagic marlstones; clayey limestone and claystones, dark gray/green in color; and distal-bathyal calcareous and siliciclastic thin-bedded microturbidites (Pl. 1). Minor isolated elements with more exotic lithologies, black chert or brecciated marly limestones, also occur. Some thicker and continuous, homogeneous sediment intervals were recovered from Unit IV: 80 cm in Hole 897C (Core 149-897C-64R), 3 m in Hole 897D (Core 149-897D-8R) and less than 25 cm in Hole 899B.

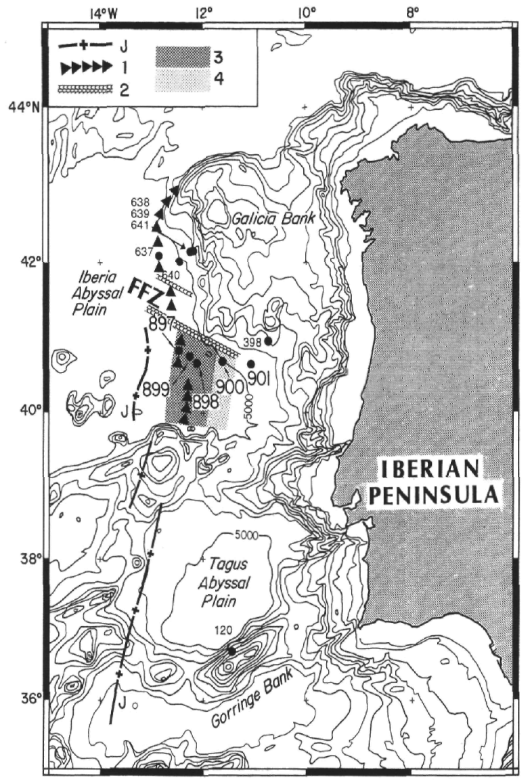

Figure 1. The Western Iberian Margin. Bathymetry after Lallemand et al.; (1985); contours in meters, bold lines are at 1000-m intervals. J = J (M0) chron. 1 = segments of peridotite ridge after Beslier et al. (1993). 2 = FFZ, or the Figueiro fault zone after Whitmarsh et al. (1990). 3,4 = transitional crust. 3 = unroofed mantle rocks exposed at the seafloor by Aptian time. 4 = synrift mafic igneous rocks exposed at the seafloor. Boundary between 3 and 4 is hypothetical. DSDP and ODP sites in the area are indicated by solid circles.

Although the lithotypes are not particularly illustrative, some features of these rocks, such as degree of consolidation, synsedimentary deformation, resedimentation and reworking, provide insights into the behavior of the source area and coeval sedimentary processes. Most of the sediments of Unit IV were already structured, cemented, or consolidated before accumulation, and preexisting pervasive microfaulting is evident in cemented or semiconsolidated microturbidites. Signs of reworking also exist (e.g., the reversed microturbidite shown in Fig. 26 of the "Site 899" chapter, Shipboard Scientific Party, 1994b). Sediments and serpentinite gouges (referred to as serpentinite "sand" by the Scientific Shipboard Party, 1994b) are intimately mixed, stretched, and sheared together (Pl. 1, Figs. 1, 4). Slump and contorted structures are common in softer lithologies. These characteristics, together with the joining of facies from different sedimentary environments, confirm the allochthonous origin of the sedimentary rock assemblage, and, in turn, of the elements of igneous rock that it includes.

Our most noteworthy conclusion from these data is that during the Aptian, coeval or nearly coeval gravity-flow and gravity-sliding deposits reached Sites 897 and 899, located about 20 km apart. This probably implies a near-flat Aptian paleotopography—basin plain setting—between these sites, and that, at this time, the "Iberia Abys-

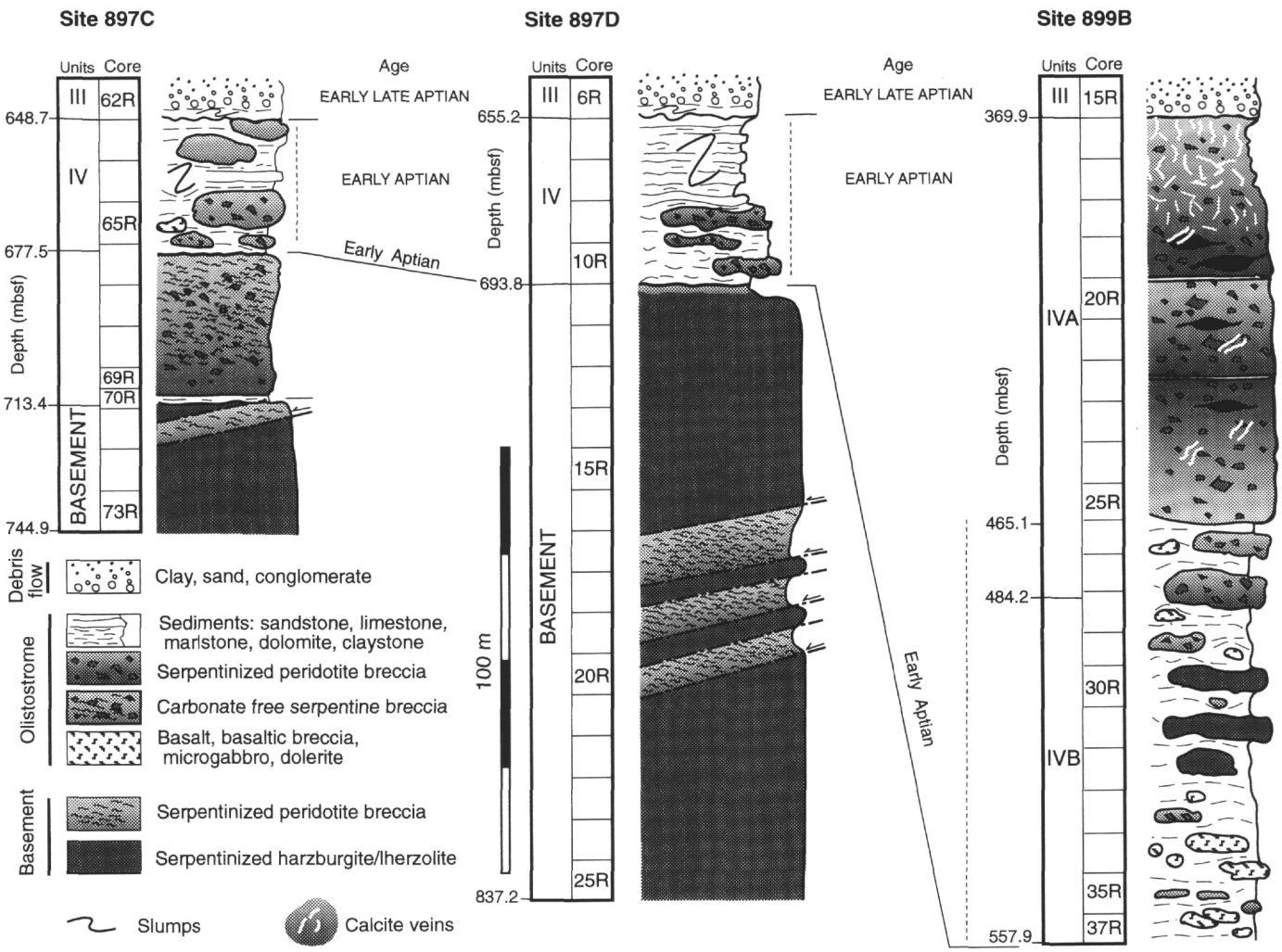

Figure 2. Diagrammatic lithologic sequences of Aptian olistostrome and peridotite basement at Sites 897 and 899. The illustration was made according to sampled lithologies and core depths, but is not keyed to recovered core intervals. Boundary of Units III and IV from Shipboard Scientific Party (1994a, 1994b). Note that sediments at Core 149-897C-70R indicate that the top of the basement is at 731.4 mbsf. For drawing clarity, veining has not been represented in smaller breccia boulders. A datum at the bottom of Unit III has been used to align the sequence.

sal Plain" (Fig. 3) was a slope-controlled sedimentary environment in which broad areas were covered by deposits derived from adjacent slopes. The absence of these deposits (Subunit IIIB and Unit IV) on the basement at Site 900 (Sawyer, Whitmarsh, Klaus, et al., 1994) indicates that in the Aptian paleogeography, the seafloor at Site 900 was higher than at Sites 897 and 899.

Because the sediments involved in the gravity-deposits are mainly of pelagic or bathyal facies, the source area for the Aptian deposits (Subunit IIIB and Unit IV) is thought to be a broad pelagic high or Seamount adjacent to the basin plain that exposed, among other rocks, older basinal sediments (Fig. 3).

From post-cruise studies we confirmed the presence of sediments in Sample 149-897C-70R-3, 26 cm. It is very important to verify the position of this sample. If correct, Unit IV would include an additional 31.5 m of peridotite breccia down to 713.4 mbsf, and the basement recovered at Hole 897C would be restricted to an interval of 31.8 m (Fig. 2).

Ages

Specific data on the abundance, preservation, and detailed range charts for the biostratigraphic distribution of Lower Cretaceous calcareous nannofossils are given in de Kaenel and Bergen (this volume).

Hole 897C

In Hole 897C, the sequence below Core 149-897C-61R (Fig. 2) contains intervals barren of nannofossils; however, some other samples include many mixed nannofossil assemblages. At the base of Subunit IIIB, Samples 149-897C-62R-4, 38 cm, 62R-4, 50 cm, and 62R-4, 60 cm, lack the Aptian markers and contain a high percentage of reworked Hauterivian to lower Barremian species. The dominance of *Nannoconus* spp. and *Micrantholithus* spp. and the absence of upper Aptian species in Section 149-897C-62R-4 indicate that the entire assemblage was reworked from older sediments.

Sample 149-897C-62R-CC, 16 cm, is assigned to the upper Aptian *R. angustus* Subzone (CC7b). An early late Aptian age for this sample is indicated by the presence of *Rhagodiscus pseudoangustus* and *Calcicalathina* sp.

The interval from Samples 149-897C-63R-1, 1 cm, to 66R-1, 10 cm is placed in the *Hayesites irregularis* Subzone (CC7a). Assemblages of this Subzone indicate an early Aptian age for this interval.

Sample 149-897C-70R-3, 26 cm, contains *Rhagodiscus achlyostaurion, Zygodiscus elegans, Flabellites oblongus* (early morphotype), and lacks *Hayesites irregularis.* This assemblage indicates the upper Barremian *R. achlyostaurion* Subzone (CC6b). This sample collected from the *JOIDES Resolution,* was from a dark, thin claystone interval mixed with serpentinite gouge, between massive ser-

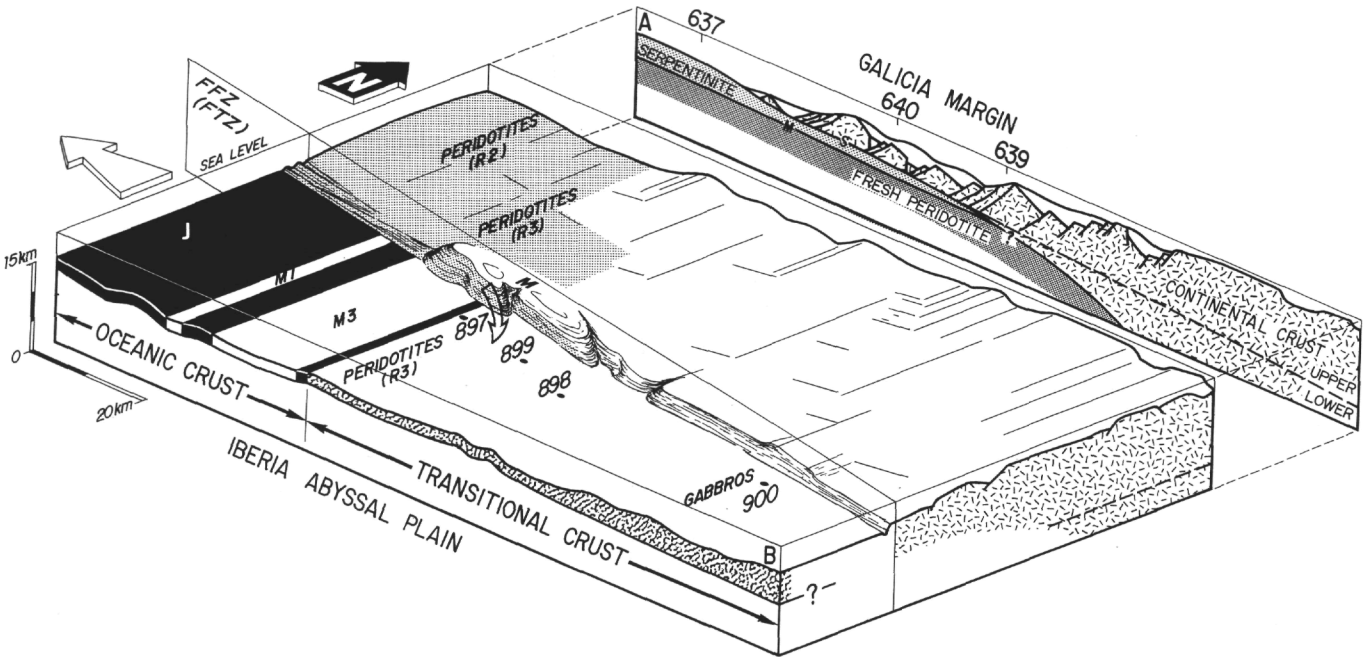

Figure 3. Cartoon paleogeographic restoration of the Western Iberian Margin during the J (M0) chron. A = crustal section across the Galicia Margin (after Boillot et al., in press, slightly modified; S = S reflector, M = Moho). B = crustal section of the Iberia Abyssal Plain, showing magnetic model from Whitmarsh et al. (1990), and transitional crust after Whitmarsh et al. (1993) (M1 and M3 = chrons). R2 and R3 = segments of peridotite ridge after Beslier et al. (1993). FEZ = Figueiro Fault Zone from Whitmarsh et al. (1990); FTF= Figueiro Transfer fault. M = position of the hypothetical marginal ridge. ODP Leg 103 sites, across the Galicia Margin, and ODP Leg 149 sites in the Iberia Abyssal Plain (IAP) are shown. The drawing is not to scale in a north-south direction. Note that the east-west section of the IAP has been shortened by 20% to compensate for post-Aptian extension produced by normal faulting.

pentinite breccias. It is the only Leg 149 sample that yielded a late Barremian nannofossil assemblage. However, it is not clear from our data if these sediments are reworked.

Middle Aptian sediments were not present in Hole 897C.

Hole 897D

In Hole 897D (Fig. 2) samples are barren or contain highly diverse, poorly to moderately well-preserved nannofossil assemblages.

Sample 149-897D-6R-3, 28 cm, at the base of Subunit IIIB, is assigned to Subzone *R. angustus* (CC7b). Nannofossil assemblages in this sample indicate an early late Aptian age. In Hole 897D, the base of the upper Aptian is placed in Sample 149-897D-6R-CC, 3 cm.

The underlying interval, down to Sample 149-897D-10R-4, 139 cm, is assigned to the lower Aptian *H. irregularis* Subzone (CC7a). The bottom of this interval (Sample 149-897D-10R-4, 139 cm) contains *Rhagodiscus achlyostaurion* and *Flabellites oblongus* (early morphotype) but lacks *Rhagodiscus angustus.* The latter species is observed 48 cm above this sample. *Hayesites irregularis* has an inconsistent occurrence in Hole 897D, since its first occurrence (FO) is recorded 170 cm above the FO of *Rhagodiscus angustus.* All these events are recorded in two cores and represent a very short period of time. Consequently, the base of this interval is placed in the same CC7a Subzone (lower Aptian), even though the zone marker (FO of *H. irregularis)* is not recorded at the same level.

As in Hole 897C, nannofossil assemblages of middle Aptian age are not present.

Hole 899B

In Hole 899B (Fig. 2), the uppermost sedimentary sample from Subunit IIIB (Sample 149-899B-26R-1, 85 cm) has a nannofossil assemblage that includes the FO *of Braarudosphaera bigelowii* and *Vagalapilla* sp. This nannofossil assemblage lacks *Eprolithus floralis* and *Palaeopontosphaera* sp. and the markers of the upper Aptian. The FO *of Rhagodiscus angustus* is in Sample 149-899B-33R-1, 12 cm. Nannofossil assemblages from the base of this sedimentary interval, Sample 149-899B-35R-1, 99 cm, contain *Hayesites irregularis, Flabellites oblongus, Rhagodiscus achyostaurion,* and *Zygodiscus elegans.*

Below the 90 m thick main interval of serpentinized peridotite breccia (termed "Upper Breccia" by Shipboard Scientific Party, 1994b) sedimentary intervals are barren of nannofossils, or contain poorly to moderately well-preserved assemblages that allow us to assign these deposits to the lower Aptian *H. irregularis* Subzone (CC7a).

The succession of nannofossil events found at Site 899 correlates and confirms those determined at Site 897. The presence *of Hayesites irregularis* below the FO of R. *angustus* found at Hole 899B confirms the placement of the lowermost samples of Hole 897D in the lower Aptian.

PETROLOGY OF BRECCIAS AND MAFIC ROCKS AT SITE 899

Serpentinized peridotite breccias recovered at Site 899 correspond to a cemented, high-angular, monomictic dark green-to-brown breccia, composed of ultramafic material and subordinate metabasites, with clasts of different sizes. A major breccia body was recovered through an interval of 95 m (Subunit IVA, Upper Breccia, Shipboard Scientific Party, 1994b) from Cores 149-899B-16R to 25R. Smaller breccia elements are intercalated with sediments, mafic rocks (basaltic lavas, fine-grained, undeformed microgabbros, sheared gabbros and fine-grained chlorite schists), and large blocks (maximum length in core of around 1.5 m) of un-

brecciated and fresh peridotite downsection to total depth (Subunit IVB) (Fig. 2).

Ultramafic Rocks

The ultramafic rocks inside the breccias (boulders, clast and fragments) vary in both composition and degree of alteration, and range from serpentinized peridotites to relatively fresh harzburgite and lherzolite (Cornen et al., this volume). Serpentine clasts are mainly composed of lizardite and magnetite, and display mesh, hourglass and bastite textures (Wicks and Whittaker, 1977). Some clasts containing metamorphic minerals such as tremolite and chlorite (clinochlore) occur locally. Within the fresh peridotite elements, minerals are finely hatched by microfractures (Sample 149-899B-19R-3, 9–14 cm), and serpentine minerals develop mainly in funnels that are zoned and composed of several generations of serpentine formed at different temperatures (Agrinier et al., this volume). None of these peridotites appears to have undergone more than greenschist grade metamorphism.

Mafic Rocks

Lavas and Undeformed Microgabbros

Fragments and clasts of undeformed microgabbros and basalts associated with sediments were recovered in the lower section of Hole 899B (Subunit IVB, from Core 149-899B-26R to 37R at total depth, Fig. 2). Aside from rare microgabbro clast, these rocks were not found inside the ultramafic breccia of Unit IVA. The basaltic rocks display porphyritic, intergranular or variolitic textures, the latter implying an emplacement onto the seafloor. The microgabbros mostly display equant textures. Though not metamorphosed, most of these rocks are deeply altered (clays and adularia).

According to their mineralogy (Ca, Ti-rich clinopyroxene, kaersutite or Ti-richterite, and biotite in the groundmass) and geochemistry, the variolitic, intergranular basalts and microgabbros have alkaline affinities. The porphyritic basalts recovered (Sample 149-899B-27R-1, 27–30 cm), which exhibit former olivine phenocrysts, Ca-rich plagioclase and titanomagnetite, have tholeiitic composition. Their origin is discussed elsewhere (Cornen et al., this volume). Such close association of different magmas has already been identified in the Galicia Margin (Kornprobst et al., 1988).

Metabasite Clasts and Boulders

Clasts of metabasite up to 10 cm in diameter are included within the serpentinite breccias at Site 899 from Core 149-899B-16R to 25R, and they form a minor component of the breccia (<5% of the clasts). Two main types of clast were found:

Type 1: metabasite clasts with a formerly porphyritic microgranular texture. They are mainly composed of prehnite and chlorite and, locally, pyroxenes, amphiboles and oxide remnants. In these clasts, feldspar has been entirely replaced by prehnite (Samples 149-899B-20R-1, 131–134 cm, 23R-3, 17–20 cm, and 27R-2, 7–11 cm). The compositions of the pyroxenes and the oxide remnants have similarities with those of the equant alkaline gabbros found in Hole 899B (from Core 149-899B-26R downsection). The unusual presence inside poikilitic prehnite of a tight microfracturation is probably related to rapid decompression. No pumpellyite was found in these prehnite-bearing rocks and the P-T conditions of the metamorphism, inferred from the mineralogical assemblages, are in the range of 200° to 400°C with a maximum pressure of 0.22 GPa (Liou et al., 1985).

Type 2: metabasite clasts with an equant association of chlorite and titanite. Boulders of similar but schistose rocks were recovered at the base of Hole 899B. They also locally show the presence of rutile, apatite, zircon, and hydrogarnet. The widespread chlorite with a bright blue interference color is a ripidolite. These rocks are exactly similar to those sampled on the Galicia Margin at the top of the peridotite section. They are interpreted as a Fe-Ti gabbro that was later sheared and metamorphosed under greenschist facies conditions (Schärer et al., 1995).

Boulder of Sheared Amphibolites

The fragments (up to 20 cm maximum size) of sheared mafic rocks found at the base of Hole 899B (lower part of Subunit IVB) are strongly foliated amphibolites. They are mainly composed of plagioclases and brown and green amphiboles, replacing clinopyroxene, with accessory green spinels (pleonaste). The assemblage of magnesio-hornblende and chlorite after pargasite (brown amphibole) and spinel is indicative of a retrogressive metamorphism from high amphibolite down to a low amphibolite to greenschist grade. The sheared texture and the mineralogy evoke former flaser-gabbros. Trace-element chemistry shows that these amphibolites are also similar to the flaser gabbros recovered to the east in Hole 900A. The composition of the Site 900 gabbros (slightly differentiated and enriched, in comparison to gabbros with MORB affinities), their degree of metamorphism, and the 136 Ma age of the last deformation event, agree well with a synrift underplated origin (Cornen et al., this volume; Féraud et al., this volume).

FABRICS OF THE SERPENTINIZED PERIDOTITE BRECCIAS AT SITE 899

Fabrics present in the serpentinized peridotite breccia are identical on both mesoscopic and microscopic scales (Pls. 2–4). The breccia is cohesive, disorganized, and highly angular, with a porphyroclastic texture. Except for few samples, no preferred orientation of clasts is observed, and a randomly oriented fabric prevails. Fragment and particle size ranges from decimetric to microscopic. The fragments can be fitted together, indicating no rotation or shear between fragments. Frequently, fragments of serpentinite cannot be clearly distinguished from the matrix or groundmass, which suggests that the matrix is generated by comminution and alteration of the serpentinized peridotite porphyroclasts. Porphyroclast sections show sharp angular edges and are frequently grouped as obviously derived from a single porphyroclast (Fig. 4). In some samples porphyroclasts are formed from deformed serpentinites or former serpentine breccia. Polyphase cracks are pervasive and can be clearly observed throughout the breccia intervals.

On the basis of the aforementioned fabric characteristics and of the specific microscopic textures and structures described below, we consider the serpentinite peridotite breccia to be a cataclasite (Twiss and Moores, 1992; Marshak and Mitra, 1988).

Serpentinized peridotite breccias and cataclasites are extensively veined on meso- and microscopic scale (Pl. 2). Vein infilling is made up of carbonates (mainly low-Mg calcite) and fibrous serpentine. This serpentine veining, similar to that encountered in the calcite-free serpentinized peridotite breccia at Site 897 (from Cores 149-978C-66R to 70R, and from Cores 149-897D-16R to 20R; Shipboard Scientific Party, 1994a), is abundant inside serpentinized peridotite boulders, clasts and fragments. It may also coexist with calcite in thicker veins that bound bigger serpentinite boulders within the breccia (Pl 2, Fig. 6). Porphyroclasts that include inherited serpentine veins are common (Pl. 2, Figs. 1–3).

Calcite veining is higher in the upper part of the breccia sequence (Upper Breccia in Unit IV, Shipboard Scientific Party, 1994b) and increases dramatically in breccia clasts included among the sediments

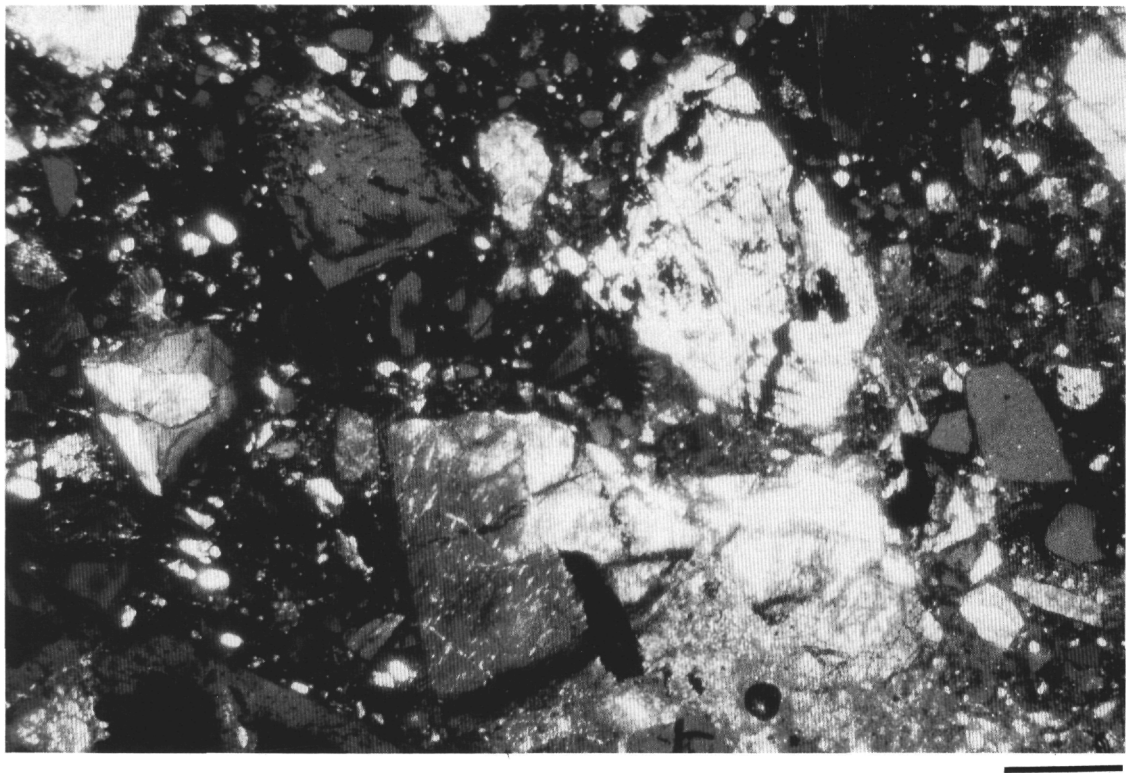

Figure 4. Sample 149-897C-66R-4, 50-55 cm. Deformational phase F_1. Thin-section photomicrograph of cataclastic texture in a calcite-free serpentinized peridotite breccia. Scale bar = 1 mm.

at the bottom of the recovered sequence (from Core 149-899B-26R downhole).

We observed three main types of vein geometry:

1. Roughly orthogonal vein sets cross-cutting porphyroclasts and matrix (Pl. 2, Figs. 1,3,4).
2. Planar crack-like thick veins. These veins usually develop antiaxial fillings that show several screens of wall rock from multiple crack-seal events, and large lateral branches (Pl. 2, Figs. 4,6).
3. A complex network of veins bounding angular porphyroclasts or breccia fragments (Pl. 2, Figs. 5, 6). This network is similar to the jigsaw puzzle pattern considered diagnostic of hydraulic implosion brecciation (Sibson, 1986).

Calcite vein fillings are granular and/or spatular and possess subhedral to anhedral crystals. When crystal size increases toward the vein center, euhedral forms may occur. Crystal orientation developed perpendicular to the vein walls, thereby indicating that veins formed as tensile fractures (Pl 2, Figs. 4, 6). Neocrystallized calcite in the breccias is largely confined to veins, and very few porphyroclasts are exclusively composed of neocrystallized calcite. This suggests that episodes of formation of thick calcite veins postdate the main processes of brecciation. Samples containing up to 40% of vein filling exhibit significant alteration and calcite replacement of the host rock, suggesting fluid-rock chemical reactions.

These three types of veins are mutually cross cutting (Pl. 2), and are frequently offset by microfaults. Vein geometry is not affected by the fabric of the wall rock, indicating that the breccia, matrix, and porphyroclasts were cohesive at times of vein formation. The structure of both the serpentine- and calcite-filling provides evidence that the opening of tensional fractures was rapid relative to filling and that fluid-assisted processes produced brecciation.

Microscope studies on selected samples from Site 899 point to a two-stage, polyphase deformational history (Pls. 3, 4) in the serpentinized peridotite breccias. We recognized a first stage of deformation (stage D) in the porphyroclasts, and, in the whole breccia, identified a second stage, F, that includes three phases (F_1, F_2, and F_3) and yields the cataclastic fabrics. Deformation phases were ordered on the basis of the overprinting of structures and relationships of mineral growth, with the structures of the various phases of deformation providing insight into deformation mechanisms.

The first stage of deformation (D) resulted in serpentinization, structures of pervasive shear foliation, and the coeval development of serpentine veins. Mylonite and cataclasite textures in serpentinite clasts (Pl. 3, Figs. 1, 4), and serpentine veins also restricted to clasts (Pl. 2, Figs. 1–3), are representative of stage D deformation.

Basement samples from Holes 897C and 897D have CS structures and rotational fabrics interpreted as stage D deformation. The penetrative deformation, including the fracture cleavage, in serpentinized peridotites from Hole 897C is also interpreted to have formed during stage D (e.g., Samples 149-897C-71R-2, 22-23 cm, and 71R-2, 8–17 cm; Shipboard Scientific Party, 1994a). The discontinuous or diffuse veins filled with dark serpentinite or white chrysotile, as well as the cataclasites observed in the lower sections of Holes 897C and 897D (below 677 mbsf in Hole 897C and below 780 mbsf in Hole 897D), are also considered to be stage D deformation (Fig. 5A).

Shear foliation structures indicate a low-temperature ductile-brittle deformation of the serpentinite during stage D. Assuming a hypothetical serpentinite composed of antigorite-chrysotile-lizardite, this ductile-brittle field is thought to have developed in P-T conditions of 0.2–0.4 GPa and below 350°–500 °C (Wicks, 1984).

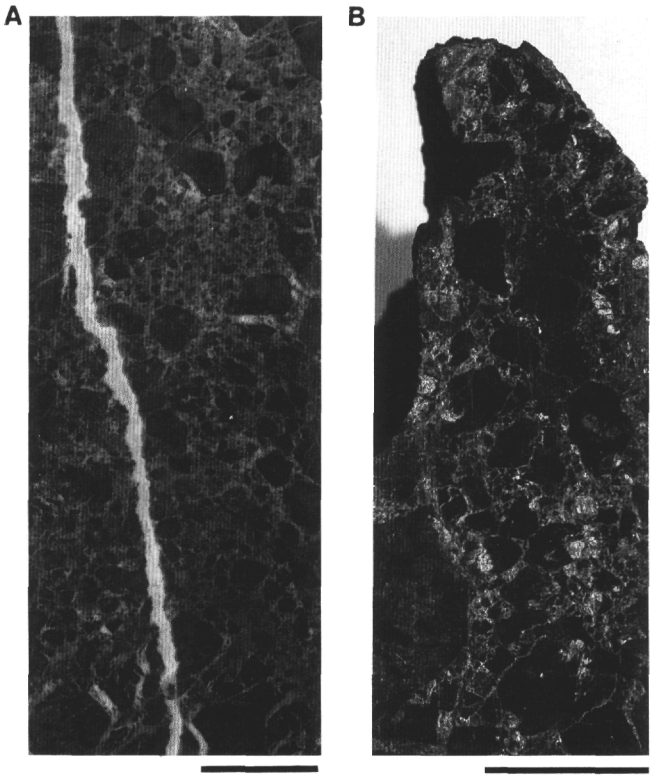

Figure 5. Hand-specimen photographs of serpentinite cataclasites (deformation stage D). **A**. Sample 149-897D-17R-4, 104–117 cm. **B**. Ronda peridotites (Betic Cordillera, southern Spain); sample was collected in a brittle fault zone south of the Ronda Massif. This sample is more cohesive than those shown in Plate 4, Figure 2. Note the similarity of the fragment angularity and fabric. In both cases the matrix is calcite-free comminuted serpentine. Scale bar = 2 cm.

The second deformation stage (F) reveals at least three main phases of brittle deformation (F_1, F_2, and F_3). The F_1 and F_2 phases of deformation resulted in structures of cataclastic brecciation (Pl. 3 and 4) and veining (Pl. 2). The F_3 deformation phase resulted in pervasive brecciation and calcite vein filling.

The F_1 deformation phase resulted in serpentinization and penetrative cataclastic fracturing, with the matrix formed exclusively by comminuted serpentine grains (Fig. 4; Pl. 3, Figs. 2–6; Pl. 4). Associated with the F_1 deformation phase, a second generation of scarce serpentine veins developed, cross-cutting the porphyroclasts and matrix. The F_1 phase cataclastic structures comprise cataclastic foliation (Pl. 3, Fig. 5) (Chester et al., 1985), cataclastic flows (see flow structures, Pl. 4, Fig. 4), and cataclastic lineation (Pl. 4, Fig. 6). To better define the cataclastic lineation (Tanaka, 1992), strain markers from oriented sections of samples from Leg 149 would have been necessary. Within the porphyroclasts, however, we recognized all the phases of cataclastic evolution (Pl. 3, Figs. 5, 6; Pl. 4, Figs. 3–5). Matrix intrusion into open fractures is common for the cataclastic lineations in the Site 899 samples, thus indicating fluid-assisted processes. Fluids favor cataclastic deformation by reducing the effective confining pressure, which leads to strain softening and hosted cataclastic flow. Cataclastic flows develop through successive cycles of softening and hardening, followed by veining and, most likely, stress corrosion and pressure solution (Babaie et al., 1991; Blenkinsop and Sibson, 1992).

The F_2 deformation phase resulted in renewed cataclastic fracturing with a matrix formed of serpentine and calcite, associated microfaults of small displacement, and cataclastic flows. No cataclastic foliation or lineation was observed for this deformation phase (Pl. 3, Figs. 2, 3).

The F_3 deformation phase shows no cataclastic features; no cataclastic lineation or flow structures have been observed. It involves pervasive fracture and veins superimposed on preexisting F_1 and F_2 phase fabrics, resulting in restocked brecciation and fractures (veins cross-cutting matrix and clasts) filled by calcite and subordinate serpentine (Pl. 2, Figs. 3–6; Pl. 3, Fig. 3).

One of the main conclusions from our fabric studies is that two major cataclastic events are recorded in the serpentinized peridotite breccias:

1. Cataclasis from stage D deformation. Fabrics from this event exist only inside clasts, boulders and intervals of serpentinized peridotite. The resulting cataclasites are associated with mylonite textures, shear foliation, and calcite-free serpentine veining.
2. Cataclasis from stage F deformation. This later, multiphasic, event resulted in serpentinization and penetrative cataclastic brecciation associated with extensive calcite and scarce serpentine veining.

Cataclasites from crystalline rocks, with fabrics similar to those of the serpentinized peridotite breccias recovered at Sites 897 and 899, are known to be formed by brittle faulting and fracturing in different tectonic settings: (1) wrench tectonics (Blenkinsop and Sibson, 1992; Tanaka, 1992; Chester et al. 1993), (2) thrusting in accretionary prisms or nappe-stacking (House and Gray, 1982), and, (3) extensional faulting (Malavieille, 1993). However, the most clear-cut examples of cataclasites have been reported from highly seismic "weak" transform fault zones (e.g., the San Andreas Fault System in southern California). In these transform zones, great amounts of overpressured fluids are found along the fault zones, and cataclasites are associated with large fracture-damage zones (Chester and Logan, 1987; Blanpied et al., 1992; Chester et al, 1993).

Well-defined examples of cataclastic fabrics in serpentinite rocks are scarce in the current literature (e.g., Hoogerduijn Strating and Vissers, 1994). Nevertheless, as the P-T conditions for brittle behavior of serpentinite rocks are below 0.15 GPa and less than 350°C (Raleigh and Paterson, 1965; Wicks, 1984), faulting below these conditions may result in serpentinite cataclasites.

In order to characterize the fault zone where the serpentinized peridotite breccias that were recovered during Leg 149 would have originated, we include examples of tectonic cataclasites from the subcontinental peridotites of the Ronda Massif (Betic Cordillera, Spain). The hand-specimen samples shown in Fig. 5B and Pl. 4, Fig. 2, belong to tabular decametric bodies of serpentinized peridotite breccias cropping out in a brittle fault zone to the south of the Ronda Massif (Sánchez-Gómez et al., 1995). This serpentinized peridotite breccia has cataclastic fabrics identical to those of the serpentinite breccias from Sites 897 and 899, and comprises a similar wide range of clast sizes; it has also recorded several phases of cataclastic deformation (Pl. 4, Fig. 2). At the outcrop, the cataclasite zone includes elements of undamaged peridotite up to 1 m in diameter that make up more than 30% of the entire rock. High-displacement narrow shear zones bound cataclasite elements, less damaged serpentinite blocks, and peridotite gouges. This assemblage of fault rocks can be observed in a zone about 200 m wide.

OLISTOSTROMES

The lower Aptian lithologic assemblages at Sites 897 and 899, which include serpentinized peridotite breccias and igneous and sedimentary rocks, are here conceived and described as an olistostrome (Fig. 2). Our interpretation is based on inferred transport mechanisms and depositional setting criteria, the range of sediment ages, and, to a

great extent, on our interpretation of the origin of the serpentinized peridotite breccias.

Since the work of Abate et al. (1970), the term olistostrome (sometimes called "gravitational mélange") has been widely used in the Alpine and Tethyan literature. It usually denotes large, thick, heterogeneous stratiform units that accumulated somewhat chaotically as a result of tectonically induced massive gravitational sliding, that is, from an active fault escarpment, in different tectonic settings (Füchtbauer and Richter, 1983). The transport distance for the sliding can vary from several dozen up to several hundred kilometers (Einsele, 1992). Olistostromes may contain large blocks called olistoliths, from several meters up to several hundreds of meters thick, that preserve their internal coherence and in which the original facies can still be established. In the displacement of the olistostromes, sliding materials can move as a more or less rigid plug through a basal shear zone (Lowe, 1982; Stow, 1986). In slide masses composed of hard rocks and semi-indurated and soft sediments, softer and friable materials make up the basal mobile phase, which may have even been liquefied and then disintegrated progressively during displacement. In contrast, hard rock elements, traveling in a passive phase in the flow, can maintain their original coherence. Because liquefaction may be restricted to the base and periphery of a large volume of slide material, most of the elements in the olistostrome may not be subject to any type of mechanical differentiation.

On the basis of the olistostrome characteristics indicated thus far, we interpret the lower Aptian lithologic complex (Unit IV) sampled at Sites 897 and 899 as follows:

1. The drilled intervals of serpentinized peridotite breccia are believed to be single bodies of former breccia that were involved in gravitational sliding (Fig. 2). Intervals of breccias up to 5 m that preserve their internal coherence and original petrology and fabric (that is, olistoliths) were recovered in Hole 897C from Sections 149-987C-66R-1 to 70R-3, and in Hole 899B from Cores 149-899B-16R to 25R. Intervals of serpentinized peridotite recovered in Hole 897C from Core 149-897C-63R to 65R, in Hole 897D from Core 149-897D-10R, and in Hole 899B from Cores 149-899B-26R to 31R are also considered boulders or clasts included in the olistostrome. From drilling data we can discern a possible major olistolith about 95 m thick (the Upper Breccia named by Shipboard Scientific Party, 1994b). However, incomplete recovery obscures whether this interval corresponds to a single body and prevents us from discussing the maximum size of olistoliths and boulders.
2. The different original sizes of breccia elements influenced the preservation of the original fabrics. Smaller elements, clasts, or fragments included in sediments at Site 899 from Core 149-899B-26R downhole were crushed and extensively altered during the transport process. In general, this alteration resulted in the replacement of the original clast mineralogy by calcite and the intrusion of sediments into the serpentinized peridotite breccia (Pl. 1, Figs. 1, 2).
3. Contorted and fractured heterogeneous sediments, cracked serpentinite breccias, and serpentinite gouges mixed with serpentine boulders and clasts (Hole 897C from Cores 149-897C-63R to 65R, and Hole 897D from Cores 149-897D-7R to 10R) are interpreted as the plastic and mobile phase in the olistostrome, which contains a record of the deformational fabrics generated during transport. The intervals of highly altered and rounded clasts of mafic rock mixed with sediment, recovered at Site 899 (from Core 149-899D-26R downhole), may also be regarded as a mobile and deformed phase in the olistostrome. Pebbles and clasts of mafic igneous rocks are believed to be reworked, altered, and disintegrated residual elements from a major volume of igneous rock originally involved in the sliding mass.
4. Shear zones affecting sediments and peridotite gouges (Cores 149-897C-65R and 897D-10R) and the sheared boundaries of olistoliths (top of Core 149-899B-16R) are interpreted as the result of deformation during the emplacement of the olistostrome. The latest generation of calcite veining, which crosscuts sediment and serpentinite lithologies (Core 149-897C-65R) or bounds bodies of different rheology (thick dipping calcite veins in Hole 899B from Cores 149-899B-17R to 25R; see Sawyer, Whitmarsh, Klaus, et al., 1994, pp. 518-526), can be interpreted as having originated from fractures that occurred in the sliding mass during transport over a long distance across the seafloor (Pl. 2., Figs. 4, 6).
5. The source area for the olistostrome was a fault-controlled escarpment, located above a gentle slope. This escarpment exposed to the seafloor the following different lithologies: serpentinite, former serpentinite cataclasites, breccias, and fault gouges; metabasites; basalts and microgabbros, sheared amphibolites, and older sedimentary rocks. The contemporaneous (Aptian) soft sediments involved in the olistostrome could have been derived from the source area, or could be seafloor sediments that were progressively incorporated into the sliding mass during its transport.
6. The incomplete recovery of Unit IV at both sites makes it impossible to determine whether the olistostrome was formed through successive sliding events or from a single massive event.

Certain characteristics of the Aptian olistostromes at Sites 897 and 899, such as their lithologic heterogeneity, strong internal deformation, and the roundness and alteration of the clasts involved, suggest long-distance transport during the gravitational sliding. We therefore define the olistostrome as distal. This implies that the tectonically active fault escarpment that generated the sliding was located far from both Site 897 and Site 899.

Some sedimentary rock samples from olistostromes at Sites 897 and 899 (Sawyer, Whitmarsh, Klaus et al., 1994) are quite similar to the Hauterivian to late Barremian dark marlstones and microturbidites recovered at Site 638 (Unit IIB and III, in Boillot, Winterer, Meyer, et al, 1987), and at Site 398 (Subunit 4C, DSDP Leg 47, in Shipboard Scientific Party, 1979). Noteworthy affinities can be seen between the mafic rock associations in the olistostrome, basalts, metabasites, and underplated gabbros sampled above the peridotites in the Galicia Margin (Boillot et al., 1988; Kornprobst et al., 1988; Beslier et al., 1990).

These similarities point to the Galicia Margin, that is, to an escarpment north of the Iberia Abyssal Plain, as the probable source of these deposits. Furthermore, the alkaline affinity and non-oceanic character of the basalt fragments within the olistostrome supports this interpretation.

DISCUSSION ON PALEOGEOGRAPHY AND TECTONIC SETTING

Two possible paleo-scenarios can be envisaged to explain the presence of lower Aptian olistostromes and upper Aptian debris-flow deposits in the IAP: there was either an active normal fault near the OCT, and therefore close to the drill sites, or there was an active major fault far away from the drilled area and outside the OCT.

On the basis of our assumptions about the distal nature of the olistostrome, and based on the provenance of the rocks involved in gravitational sliding, we advocate the second scenario and we propose

that the probable source area for the olistostromes and debris-flows recovered at Sites 897 and 899 was the Figueiro Fracture Zone (FFZ) (Fig.l).

To explain our hypothesis (Fig. 3), we sketch an early Aptian palinspastic restoration of the Western Iberian Margin. This drawing displays a schematic submarine physiography that fits current crustal models for the Galicia Margin (Boillot, Winterer, Meyer, et al., 1987; Boillot et al., 1989; Boillot et al., in press) and for the Iberia Abyssal Plain (Whitmarsh et al., 1990; Whitmarsh et al, 1993). Our restoration tries to stress the differences in the character of the lithosphere of the Western Iberian Margin at the time of the J (M0) anomaly (Srivastava et al., 1990) to the north and south of the FFZ. We believe the FFZ, originally interpreted by Whitmarsh et al. (1990) as a fracture zone, may have had the character of a true transform fault zone at times when both vertical and horizontal motions between the IAP and the Galicia Margin varied along this fault zone. That is, while the generation of transitional crust and sea-floor spreading was taking place in the IAP, the adjacent Galicia continental margin was still undergoing stretching (synrift stage). The relative motion along the FFZ transform boundary should have ceased just when active sea floor spreading started on the Galicia Margin (after chron M0).

Our hypothesis centers on the importance of the Figueiro Fracture Zone (Whitmarsh et al., 1990) as a major tectonic lineament, although the existence of this fracture zone in itself is a matter of discussion (Beslier et al., 1993). The weak appearance of this fracture on some multichannel seismic profiles, however, does not rule out its presence, as vertical wrench faults are never clearly evidenced in seismic reflection profile data. Furthermore, the present evidence of this transform fault zone, given its episodic character, could easily be masked by later tectonic evolution of the Western Iberian Margin.

Wrench tectonics at the Figueiro Transform Zone (FTZ, Fig. 3), associated with a great amount of over-pressured fluids, probably caused cataclastic breccias and fault rocks and a large fracture-damaged zone in the host basement-rocks. We suggest that a marginal ridge, expressed as a tectonically uplifted area in the transform zone, would have formed to the north of an Aptian abyssal plain, just as marginal ridges are formed at transform margins (Keen et al., 1990; Mascle et al., 1988; Mascle et al., 1993) or in oceanic transform fault zones (Honnorez et al., 1994).

The cartoon in Figure 3 explains how the southern steeper escarpment of the marginal ridge (M) could have exposed at the seafloor the serpentinites, and even the underplated gabbros and magmatic rocks, of the Galicia Margin (Boillot, Winterer, Meyer, et al., 1987; Boillot et al., 1988; Kornprobst et al., 1988). Synrift sedimentary sequences of the Galicia Margin would have overlain the ultramafic rocks in the marginal ridge, and also cropped out at the escarpment. By the Aptian, all these rocks should have been deformed by the stretching of the Galicia Margin.

As a probable trace of this Aptian marginal ridge, we point to the debris-flow interval recovered at Sites 897 and 899 (reddish cobble-conglomerate, Subunit IIIB). This debris flow may have resulted from reworking of probable gravel deposits on the FTZ; like the gravels known from recent transform zones (i.e., Atlantis II Fracture Zone; Swift, 1991). Any expression of this marginal ridge could likewise have been destroyed by tectonic-gravitational denudation processes. The olistostromes drilled during Leg 149 may provide evidence of one of these tectonic-gravitational denudation event during the early Aptian.

CONCLUSION

The following conclusions can be drawn from the present work:

1. The Aptian lithologic complex recovered from the acoustic basement at Sites 897 and 899 is interpreted as olistostrome(s) that accumulated in a basin-plain setting. The intervals of serpentinized peridotite breccia are considered to be olistoliths or blocks from former tectonic breccias (cataclasites).
2. Sedimentary intervals in the olistostrome include reworked elements from the synrift sedimentary sequence of the Galicia Margin, and coeval early Aptian pelagic sediments.
3. The fabrics of the serpentinized peridotite breccias denote strong multiphase cataclasis. An earlier cataclastic event, which resulted in cataclasite associated with mylonite, shear foliation, and calcite-free serpentine veining (stage D deformation), is evidenced inside serpentinite boulders and breccia clasts. These fabrics may be related to a synrift brittle-ductile deformation in the peridotites on the Galicia Margin. A later cataclastic event that resulted in penetrative cataclastic fabrics associated with serpentinization, in extensive calcite and serpentine veining, and in restocked brecciation (multiphase stage F deformation) contributed to the whole fabric observed in the serpentinite breccia.
4. The main multiphase cataclasis (stage F) recognized in the breccia is considered to have originated from wrench tectonics in a transform fault zone. Hydrothermal circulation probably played a significant role in the fluid-assisted processes that gave way to the penetrative cataclastic fabric and to several generations of serpentine observed in the breccias.
5. We propose the Figueiro Fault Zone as the probable transform fault zone that caused the serpentinized peridotite cataclastic breccia and a tectonically active marginal ridge within that transform zone as the source area for the olistostromes.
6. The high degree of fracturing in the metamorphic gabbros (Fig. 6) recovered at Site 900, the site nearest the FTZ track, could also be related to damage from the activity of this transform-fault zone.

Post-olistostrome Block Faulting

The olistostromes at Sites 897 and 899 were cored on the top of discrete fault-bounded basement highs; this suggests tectonic uplift of these sites from a deep basinal setting in the Aptian to their present position on the top of these basement highs. This block faulting happened after the emplacement of the olistostrome and overlying debris-flow deposits and before the sediments that seal the basement highs were laid down (pelagic facies of Subunit IIIA, latest Cretaceous or early Paleocene). According to these time constraints, the normal faults that bound the ridges ought to occur at any time after the late Aptian and before the latest Cretaceous or Paleocene. At Sites 897 and 899, biostratigraphic data indicate a hiatus for these ages (Sawyer, Whitmarsh, Klaus et al., 1994). This hiatus, about 33 m.y. long, should correspond to times when the "ridges" formed submarine hills, where sediments were eroded or not deposited. It is known that post-Miocene tectonics in the Iberia Abyssal Plain favored local inversions of some of these normal faults (Sawyer, Whitmarsh, Klaus, et al., 1994).

Given the aforementioned data, and considering seafloor spreading began in the IAP at about late Hauterivian (Kent and Gradstein, 1986; Whitmarsh et al, 1990; Whitmarsh et al., 1993), our conclusion is that the "basement ridges" in the Iberia Abyssal Plain (Beslier et al., 1993) are not synrift features of this margin, but resulted from postrift normal faulting near the OCT boundary. According to the above time constraints, this postrift block-faulting probably took place post-chron M0 and pre-chron 34 (Late Cretaceous), and was perhaps related to the change of motion of Iberia relative to the neighboring Africa and America plates (Srivastava and Verhoef, 1992; Srivastava et al., 1990).

ACKNOWLEDGMENTS

M.C. Comas, G. Cornen, and E. de Kaenel would like to thank the Ocean Drilling Program for inviting them to participate in ODP Leg

149. The authors express their gratitude to L. Dearmont and A. Klaus for corrections and, to the reviewers P. Tricart, Shoji Arai, and R. Whitmarsh (ERB member) for corrections and comments. We would also like to thank the Shipboard Scientific Party, the ODP technicians, and the SEDCO drilling crew of Leg 149 for their help. Financial support for M.C. Comas and M. Sánchez-Gómez was provided by the Spanish Consortium for the ODP and Project PB91-00800-c02-01 (DGICIT). Financial support for G. Cornen was given by a CNRS grant (Geoscience Marine).

REFERENCES

Abate, E., Bortolotti, V., and Passerini, P., 1970. Olistostromes and olistoliths. *In* Sestini, E. (Ed.), *Development of the Northern Apennines Geosyncline.* Sediment. Geol., 4:521–537.

Babaie, H.A., Babaie, A., and Hadizadeh, J., 1991. Initiation of cataclastic flow and development of cataclastic foliation in nonporous quartzites from a natural fault zone. *Tectonophysics,* 200:67–77.

Beslier, M.-O., Ask, M., and Boillot, G., 1993. Ocean-continent boundary in the Iberia Abyssal Plain from multichannel seismic data. *Tectonophysics,* 218:383–393.

Beslier, M.-O., Girardeau, J., and Boillot, G., 1990. Kinematics of peridotite emplacement during North Atlantic continental rifting, Galicia, NW Spain. *Tectonophysics,* 184:321–343.

Blanpied, M.L., Lockner, D.A., and Byerlee, J.D., 1992. An earthquake mechanism based on rapid sealing of faults. *Nature,* 358:574–575.

Blenkinsop, T.G., and Sibson, R.H., 1992. Aseismic fracturing and cataclasis involving reaction softening within core material from the Cajon Pass Drill Hole. *J. Geophys. Res.,* 97:5135–5144.

Boillot, G., Beslier, M.O., Krawczyk, C.M., Rappin, D., and Reston, T.J., in press. The formation of passive margins: constraints from the crustal structure and segmentation of the deep Galicia margin (Spain). *J. Geol. Soc. London.*

Boillot, G., Comas, M.C., Girardeau, J., Kornprobst, J., Loreau, J.-P., Malod, J., Mougenot, D., and Moullade, M., 1988. Preliminary results of the Galinaute cruise: dives of the submersible *Nautile* on the Western Galicia Margin, Spain. *In* Boillot, G., Winterer, E.L., et al., *Proc. ODP, Sci. Results,* 103: College Station, TX (Ocean Drilling Program), 37–51.

Boillot, G., Fèraud, G., Recq, M., and Girardeau, J., 1989. "Undercrusting" by serpentinite beneath rifted margins: the example of the west Galicia margin (Spain). *Nature,* 341:523–525.

Boillot, G., Winterer, E.L., Meyer, A.W., et al, 1987. *Proc. ODP, Init. Repts.,* 103: College Station, TX (Ocean Drilling Program).

Chester, F.M., Evans, J.P., and Biegel, R.L., 1993. Internal structure and weakening mechanisms of the San Andreas Fault. *J. Geophys. Res.,* 98:771–786

Chester, F.M., Friedman, M., and Logan, J.M., 1985. Foliated cataclasites. *Tectonophysics,* 111:139–146.

Chester, F.M., and Logan, J.M., 1987. Composite planar fabric of gouge from the Punchbowl Fault, California. *J. Struct. Geol.,* 9:621–634.

Einsele, G., 1992. *Sedimentary Basins:* Berlin (Springer-Verlag).

Füchtbauer, H., and Richter, D.K., 1983. Relations between submarine fissures, internal breccias and mass flows during Triassic and earlier rifting periods. *Geol. Rundsch.,* 72:53–66.

Honnorez, J., Villeneuve, M., and Mascle, J. 1994. Old continent-derived metasedimentary rocks in the Equatorial Atlantic: an acoustic basement outcrop along the fossil trace of the Romanche transform fault at 6°30'W. *Mar. Geol.,* 117:237–251.

Hoogerduijn Strating, E.H., and Vissers, R.L.M., 1994. Structures in natural serpentinite gouges, *J. Struct. Geol.,* 16:1205–1215.

House, W.M., and Gray, D.R., 1982. Cataclasites along the Saltville thrust, USA, and their implications for thrust-sheet emplacement. *J. Struct. Geol.,* 4:257–269.

Keen, C.E., Kat, W.A., and Roest, W.R., 1990. Crustal anatomy of a transform margin. *Tectonophysics,* 173:527–544.

Kent, D.V., and Gradstein, F.M., 1986. A Jurassic to Recent chronology in the western North Atlantic region. *In* Tucholke, B.E., and Vogt, P.R. (Eds.), *The Geology of North America* (Vol. 1): *The Western Atlantic Region.* Geol. Soc. Am., 45–50.

Kornprobst, J., Vidal, P., and Malod, J., 1988. Les basaltes de la marge de Galice (NO de la Péninsule Ibérique): hétérogénéité des spectres de terres rares à la transition continent/océan. Données géochimiques préliminaires. *C.R. Acad. Sci. Ser. 2,* 306:1359–1364.

Lallemand, F., Maze, J.P., Marti, P., and Sibuet, J.C., 1985. Présentation d'une carte bathymétrique de l'Atlantique nord-est. *C.R. Acad. Sci. Ser. 2,* 300:145–149.

Liou, J.G., Maruyama, S., and Cho, M., 1985. Phase equilibria and mineral parageneses of metabasites in low-grade metamorphism. *Mineral. Mag.,* 49:321–333.

Lowe, D.R., 1982. Sediment gravity flows: II. Depositional models with special reference to the deposits of high-density turbidity currents. *J. Sediment. Petrol.,* 52:279–297.

Malavieille, J., 1993. Late orogenic extension in mountain belts: insights from the Basin and Range and the late Paleozoic Variscan Belt. *Tectonics,* 12:1115–1130.

Marshak, S., and Mitra, G., 1988. *Basic Methods of Structural Geology:* Englewood Cliffs (Prentice-Hall).

Mascle, J., Blarez, E., and Marinho, M., 1988. The shallow structures of the Guinea and Côte d'Ivoire-Ghana transform margins: their bearing on the equatorial Atlantic Mesozoic evolution. *Tectonophysics,* 155:193–209.

Mascle, J., Guiraud, M., Basile, C., Benkhelil, J., Bouillin, J.P., Cousin, M., and Mascle, G., 1993. The Cote d'Ivoire-Ghana transform margin: preliminary results from the *Equanaute* cruise (June 1992). *C.R. Acad. Sci. Ser. 2,* 316:1255–1261.

Mauffret, A.,Mougenot, D., Miles, P.R., and Malod, J.A., 1989. Cenozoic deformation and Mesozoic abandoned spreading centre in the Tagus abyssal plain (west of Portugal): results of a multichannel seismic survey. *Can. J. Earth Sci.,* 26:1101–1123.

Pinheiro, L.M., Whitmarsh, R.B., and Miles, P.R., 1992. The ocean-continent boundary off the western continental margin of Iberia, II. Crustal structure in the Tagus Abyssal Plain. *Geophys. J.,* 109:106–124.

Raleigh, C.B., and Paterson, M.S., 1965. Experimental deformation of serpentinite and its tectonic implications. *J. Geophys. Res.,* 70:3965–3985.

Sánchez-Gómez, M., García-Dueñas, V., Muñoz, M., and Balanyá, J.C., 1995. Relación estructural de los cuerpos peridotíticos situados al Norte y al Sur del Estrecho de Gibraltar. *Geogaceta.,* 17:135–137.

Sawyer, D.S., Whitmarsh, R.B., Klaus, A., et al., 1994. *Proc. ODP, Init. Repts.,* 149: College Station, TX (Ocean Drilling Program).

Schärer, U., Kornprobst, J., Beslier, M.O., Boillot, G., and Girardeau, J., 1995. Gabbro and related rock emplacement beneath rifting continental crust: U-Pb geochronological and geochemical constraints for the Galicia passive margin (Spain). *Earth Planet. Sci. Lett.,* 130:187–200.

Shipboard Scientific Party, 1979. Site 398. *In* Sibuet, J.-C., Ryan, W.B.F., et al., *Init. Repts. DSDP,* 47 (Pt. 2): Washington (U.S. Govt. Printing Office), 25–233.

———, 1994a. Site 897. *In* Sawyer, D.S., Whitmarsh, R.B., Klaus, A., et al., *Proc. ODP, Init. Repts.,* 149: College Station, TX (Ocean Drilling Program), 41–113.

———, 1994b. Site 899. *In* Sawyer, D.S., Whitmarsh, R.B., Klaus, A., et al., *Proc. ODP, Init. Repts.,* 149: College Station, TX (Ocean Drilling Program), 147–209.

Sibson, R.H., 1986. Brecciation processes in fault zones: inferences from earthquake rupturing. *Pure Appl. Geophys.,* 124:159–175.

Srivastava, S.P., Roest, W.R., Kovacs, L.C., Oakey, G., Levesque, S., Verhoef, J., and Macnab, R., 1990. Motion of Iberia since the Late Jurassic: results from detailed aeromagnetic measurements in the Newfoundland Basin. *Tectonophysics,* 184:229–260.

Srivastava, S.P., and Verhoef, J., 1992. Evolution of Mesozoic sedimentary basins around the North Central Atlantic: a preliminary plate kinematic solution. *In* Parnell, J. (Ed.), *Basins of the Atlantic Seaboard: Petroleum Geology, Sedimentology and Basin Evolution.* Geol. Soc. Spec. Publ. London, 62:397–420.

Stow, D.A.V., 1986. Deep clastic seas. *In* Reading, H.G. (Ed.), *Sedimentary Environments and Facies:* London (Blackwell Sci. Publ.), 399–446.

Swift, S.A., 1991. Gravels in the Atlantis II Fracture Zone. *In* Von Herzen, R.P., Robinson, P.T., et al., *Proc. ODP, Sci. Results,* 118: College Station, TX (Ocean Drilling Program), 431–438.

Tanaka, H., 1992. Cataclastic lineations. *J. Struct. Geol.,* 14:1239–1252.

Twiss, R.J., and Moores, E.M., 1992. *Structural Geology:* New York (Freeman).

Whitmarsh, R.B., Miles, P.R., and Mauffret, A., 1990. The ocean-continent boundary off the western continental margin of Iberia, I. Crustal structure at40°30'N. *Geophys. J. Int.,* 103:509–531.

Whitmarsh, R.B., Pinheiro, L.M., Miles, P.R., Recq, M, and Sibuet, J.C., 1993. Thin crust at the western Iberia ocean-continent transition and Ophiolites. *Tectonics,* 12:1230–1239.
Wicks, F.J., 1984. Deformation histories as recorded by serpentinites, II: Deformation during and after serpentinization. *Can. Mineral.,* 22:197–204.
Wicks, F.J., and Whittaker, E.J.W., 1977. Serpentine textures and serpentinization. *Can. Mineral.,* 15:459–488.

Date of initial receipt: 2 January 1995
Date of acceptance: 3 August 1995
Ms 149SR-228

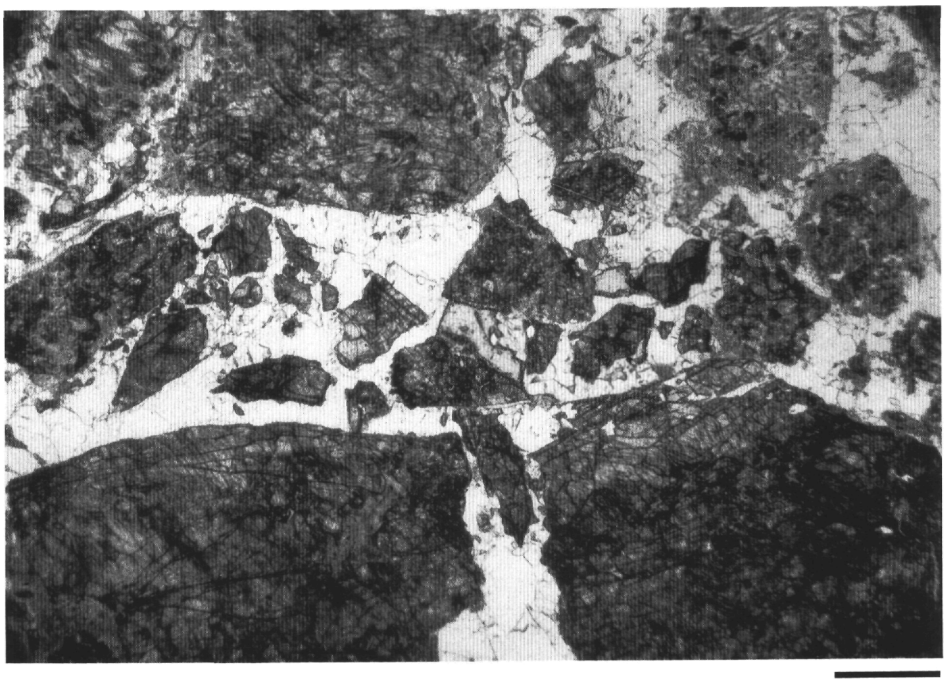

Figure 6. Sample 149-900A-85R-5, 109-114 cm. Thin-section photomicrograph showing internal breccia of highly fractured tremolite-bearing metagabbro in a thick calcite vein. Plane-polarized light. Scale bar = 1 mm.

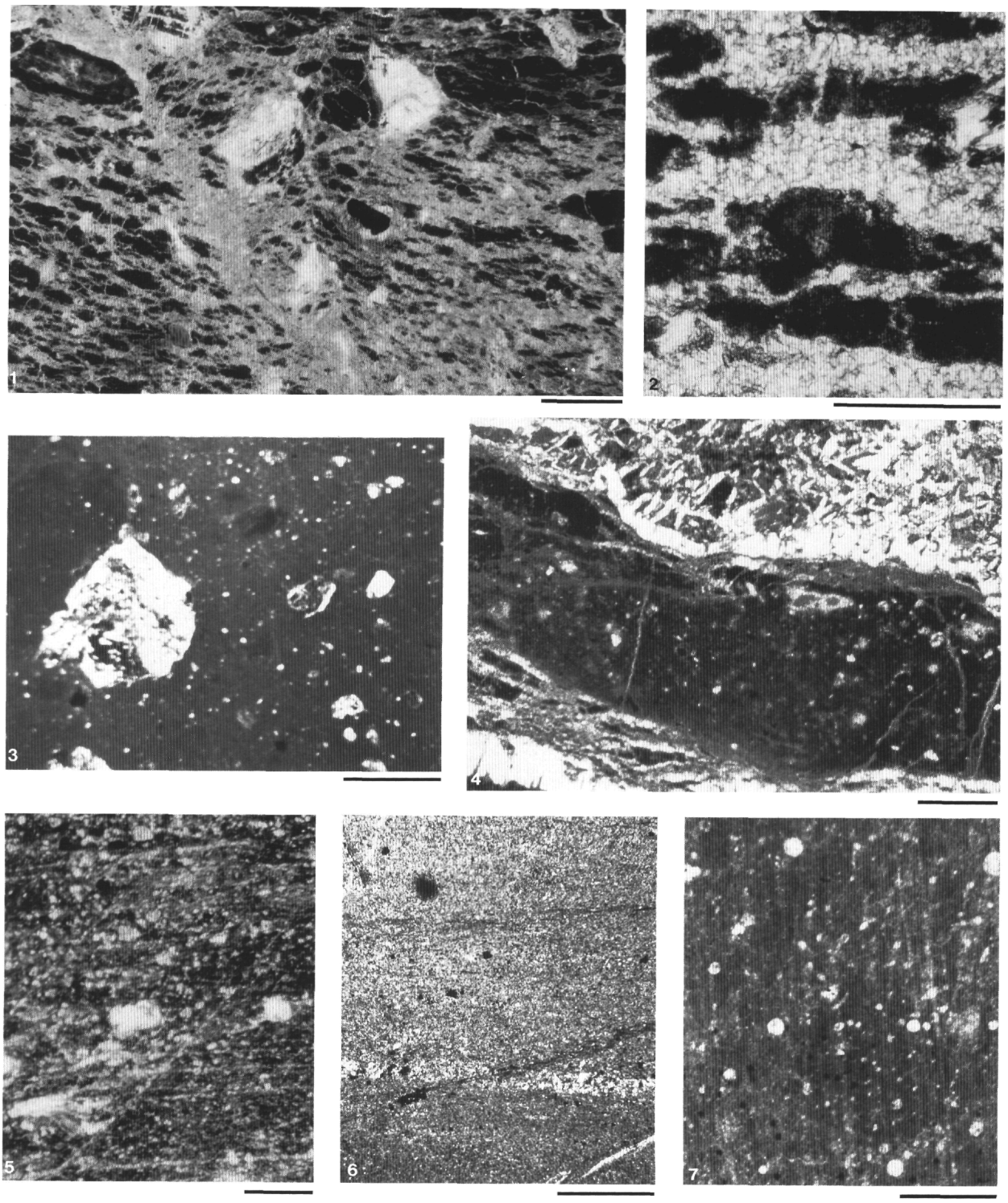

Plate 1. Thin-section photomicrographs of sediments from Sites 897 and 899, all under plane-polarized light. **1.** Sample 149-899B-27R-1, 71-73 cm. Micritic (microsparite) sediments intruding serpentinized peridotite breccia with dilatant texture. Scale bar = 500 μm. **2.** Detail of (1) showing equant dolomitized microsparite between altered serpentinite. Note features of calcite replacement. Scale bar = 100 μm. **3.** Sample 149-897D-10R-1, 43-45 cm. Fault-gouge composed of comminuted and altered peridotite fragments and clayed sediments. Scale bar = 2 mm. **4.** Sample 149-897D-10R-1, 12-15 cm. Similar serpentinized peridotite/sediment fault-gouge as in (3). Note shear zone developing calcite veins in lower left corner. Peridotite fragment in upper right corner. Scale bar = 500 μm. **5.** Sample 149-899B-35R-1, 123-129 cm. Laminated cherty silty-claystone. Scale bar = 100 μm. **6.** Sample 149-897D-9R-1, 57-59 cm. Silty carbonate cemented microturbidite; organic matter is abundant. Scale bar = 2 mm. **7.** Sample 149-899D-26R-1, 81-88 cm. Radiolarian marl (stripes are from thin-section processing). Scale bar = 2 mm.

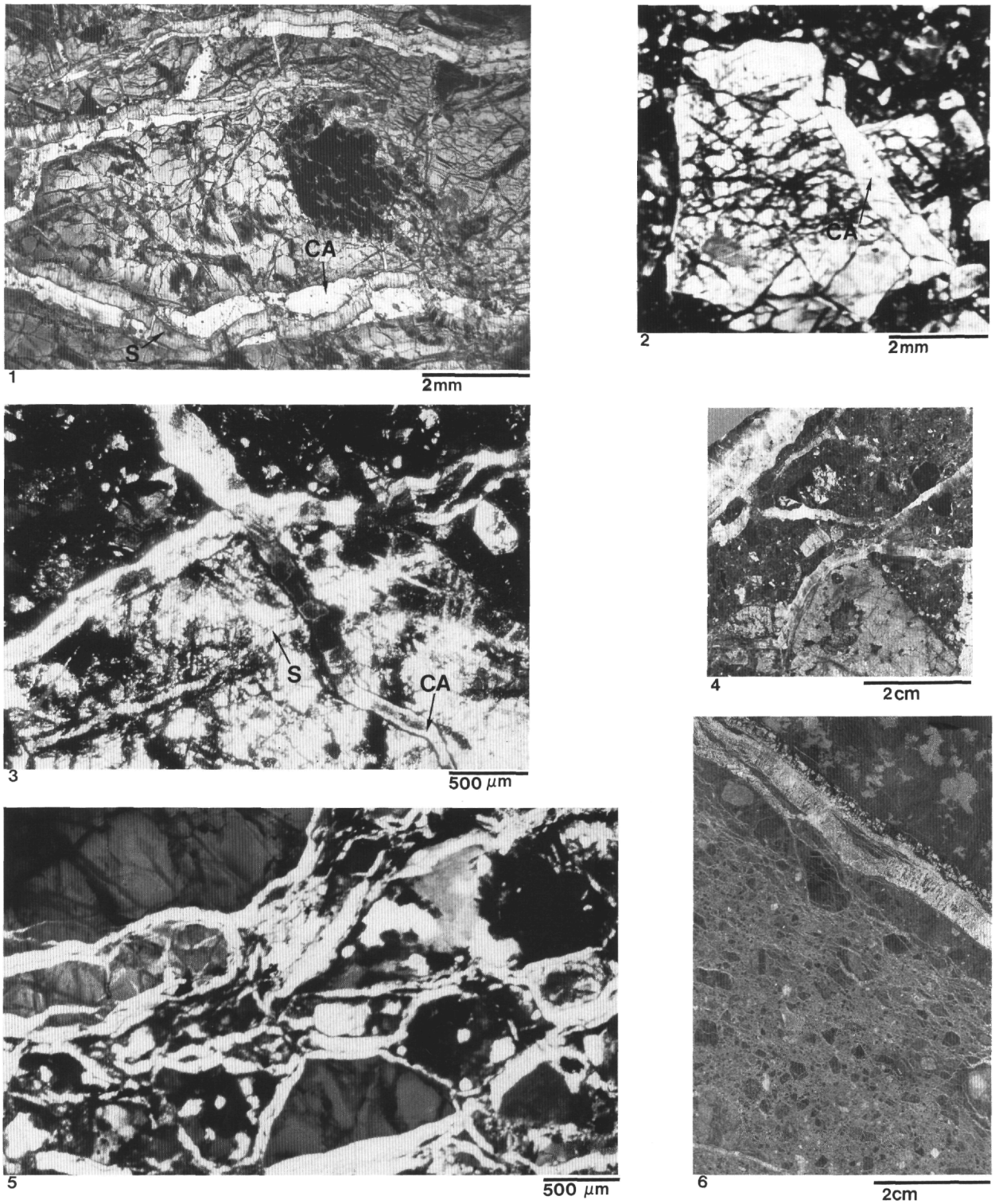

Plate 2. Calcite (deformational phase F_3) and serpentine veins (deformational stage D) from Hole 899B. **1.** Sample 149-899B-31R-1, 67-71 cm. Thin-section photomicrograph of serpentinite (S) veins overgrown by calcite (CA) within a clast of serpentinized peridotite. Plane-polarized light. **2.** Sample 149-899B-19R-1,6-11 cm. Thin-section photomicrograph of a chrysotile vein (CR) in a serpentine-magnetite clast included within a cataclastic breccia. Plane-polarized light. **3.** Sample 149-899B-18R-4, 99-110 cm. Thin-section photomicrograph of calcite veins (CA) that cross-cut the cataclastic breccia. Note calcite veins surrounding and cross-cutting large porphyroclast including serpentine veins (S). Crossed nicols. **4.** Sample 149-899B-18R-2, 39-44 cm. Hand-specimen photograph showing calcite veins that cross-cut porphyroclast and matrix. Note the absence of shear movement associated with calcite veins; note also the large "dipping" vein with antiaxial filling in the upper left corner. **5**. Sample 149-899B-16R-2, 23-27 cm. Thin-section photomicrograph showing complex network of calcite veins bounding angular porphyroclast and breccia fragments (jigsaw-puzzle pattern). **6.** Sample 149-899B-21R-2, 40-55 cm. Mesoscopic jigsaw-puzzle pattern network of calcite veins (similar to (5)) in breccia. In the upper right corner is a large calcite vein, with an antiaxial filling, bounding a relatively fresh peridotite clast. Note lateral branches of the large vein merging with the network of minute veins bounding clasts. Note weak cataclastic foliation indicative of shear between peridotite clast and breccia.

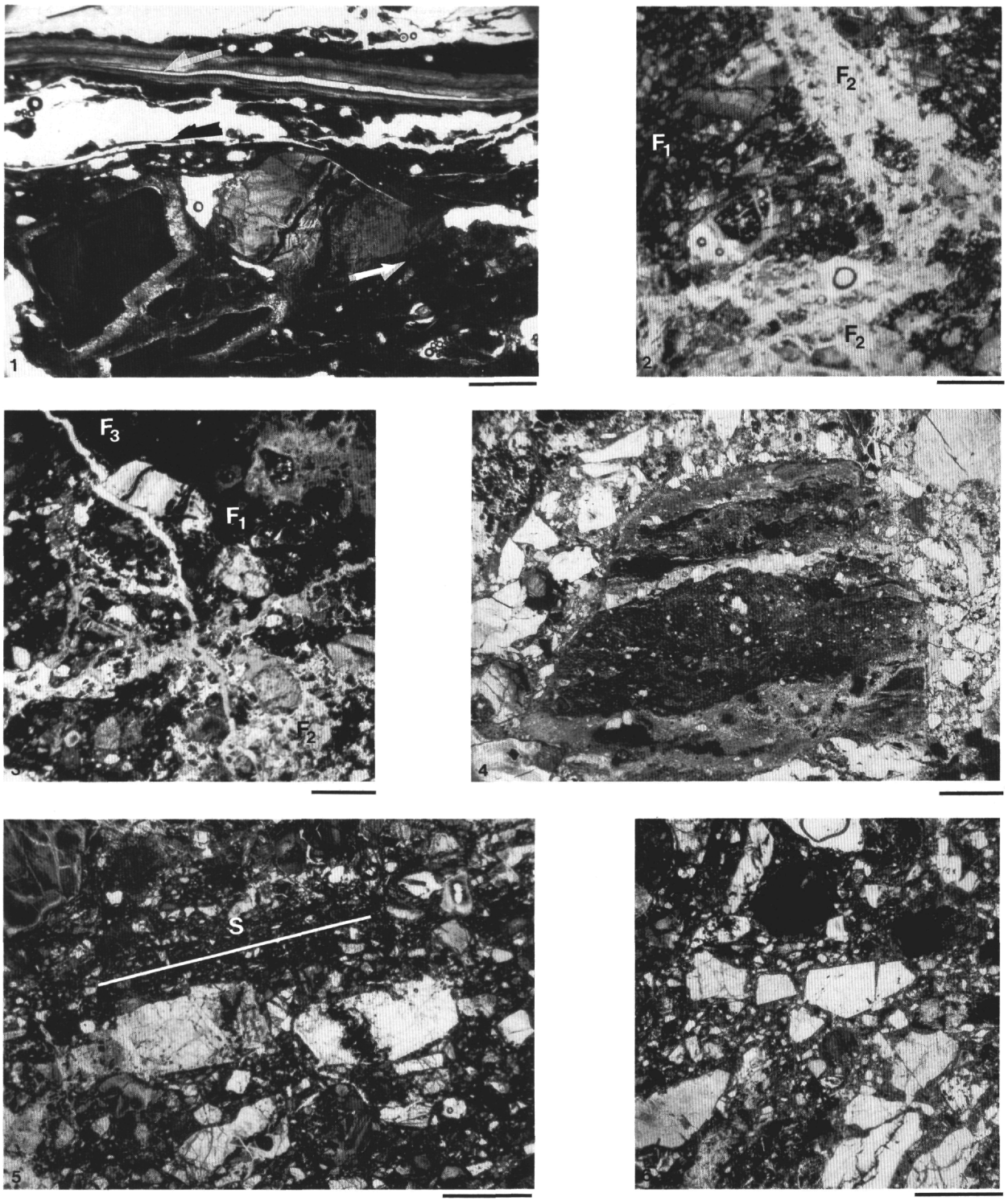

Plate 3. Thin-section photomicrographs of cataclasites from Hole 899B, all under plane-polarized light. Scale bar = 1 mm. **1.** Sample 149-899B-27R-1, 40–45 cm. Deformational stage D serpentinite mylonite. Note the serpentine σ-type porphyroclast and the serpentine fibers (parallel to top of photograph) that have grown parallel to shear. Arrows indicate the apparent shear sense. Blanks are voids produced during thin-section processing. **2.** Sample 149-899B-29R-1, 82–84 cm. Serpentinite cataclasite showing two breccia generations. Phase F_1 breccia (early breccia) consists of serpentine clasts and serpentine matrix. Phase F_2 breccia consists of phase F_1 breccia clast and serpentine-calcite matrix. **3.** Sample 149-899B-29R-1, 73-76 cm. Calcite vein (phase F_3) cross-cutting phase F_1 and F_2 breccias. **4.** Sample 149-899B-19R-2, 37-42 cm. Foliated ultracataclasite (deformational stage D) fragment within phase F_1 breccia. **5.** Sample 149-899B-29R-1, 82-84 cm. Deformational phase F_1. Broken porphyroclast consisting of serpentine and opaque mineral (magnetite?) surrounded by vague cataclastic foliation (S). All of the matrix is serpentine. Note the open crack in the porphyroclast filled by matrix. **6.** Sample 149-899B-29R-1, 43–48 cm. Porphyroclasts broken during the F_1 deformational phase. Note the different degrees of single porphyroclast breakages. Compare with Plate 4, Figures 4–6.

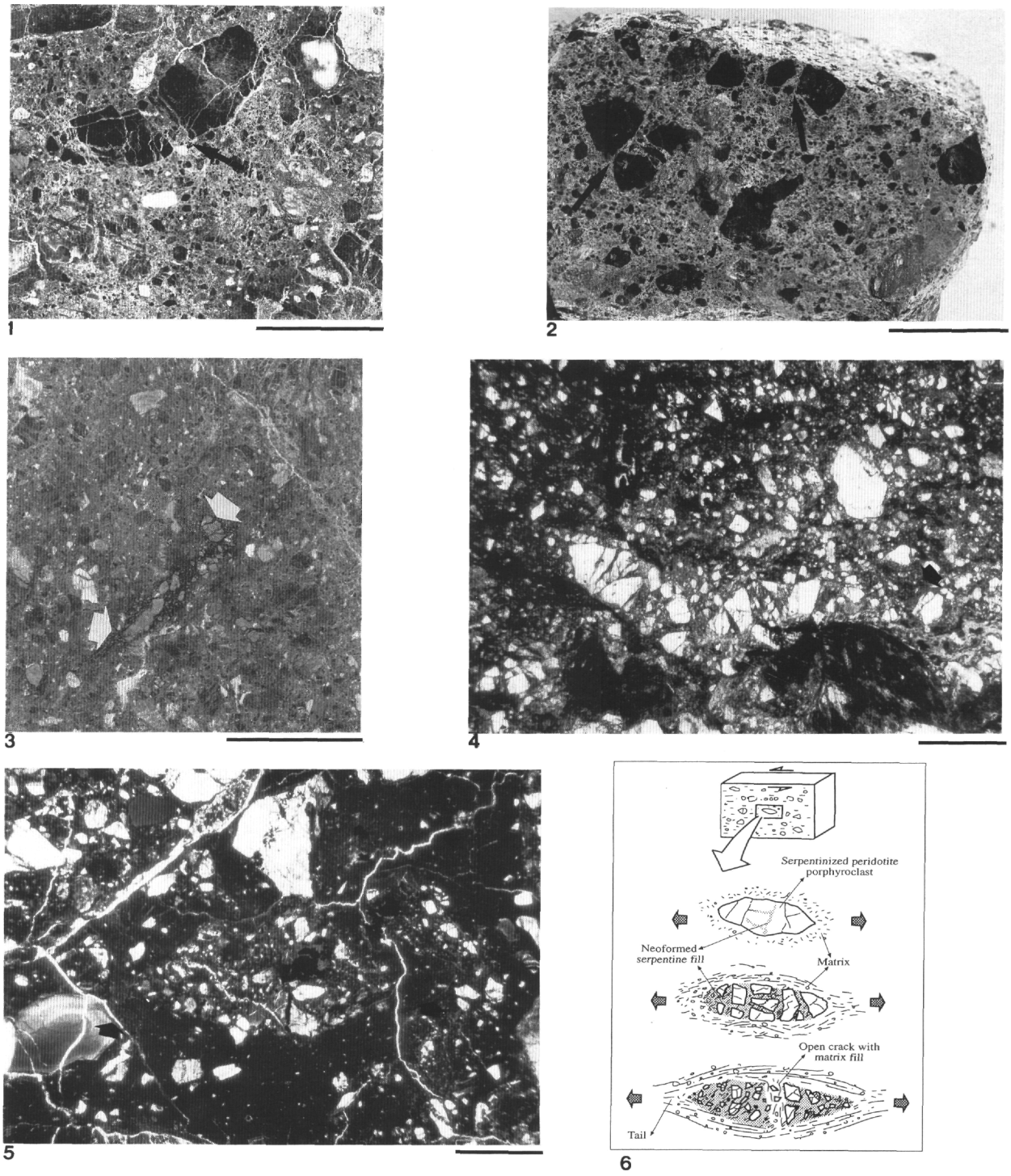

Plate 4. Cataclastic textures in phase F_1 serpentinite breccias. **1.** Sample 149-899B-21R-4, 19-25 cm. Hand-specimen photograph of serpentinite cataclasite. Both fragment types, light and dark, are made of serpentine. Note the crack fill (arrow) of the largest porphyroclast, containing grain fragments from the matrix, suggesting a fluid pathway. Scale bar = 2 cm. **2.** Hand-specimen photograph of serpentinite cataclasite from Ronda peridotites (Betic Cordillera, southern Spain). Sample is from an extensional detachment fault zone. Note the great similarity of the cracks and fills (arrows) with those of the sample from the Iberia Abyssal Plain in (1). Note also the foliated cataclasite porphyroclast in the lower right corner. Scale bar = 2 cm. **3, 4.** Compare meso- and microscopic fabric of broken elongated porphyroclasts (between arrows). (3). Sample 149-899B-26R-1, 49-55 cm. (4). Sample 149-899B-25R-3, 80-84 cm. Note neoformed serpentine fill between cracks. Plane-polarized light. (3) Scale bar = 2 cm, (4) scale bar = 1 mm. **5.** Sample 149-899B-29R-1, 43-48 cm. Flow structure around a highly broken porphyroclast consisting of serpentine and opaque mineral fragments. The veins are calcite and cross-cut all structures. Arrows indicate tails. Plane-polarized light. Scale bar = 1 mm. **6.** Suggested process of growth of cataclastic lineation observed in serpentinites at Site 899, after Tanaka (1992) but slightly modified (see text).